NASA Technical Memorandum 83791

The Effects of Seven Alloying Elements on the Microstructure and Stress-Rupture Behavior of Nickel-Base Superalloys

D. R. Hull, R. V. Miner, and C. A. Barrett
Lewis Research Center
Cleveland, Ohio

October 1984

NASA

THE EFFECTS OF SEVEN ALLOYING ELEMENTS ON THE MICROSTRUCTURE AND STRESS-RUPTURE BEHAVIOR OF NICKEL-BASE SUPERALLOYS

D. R. Hull, R. V. Miner and C. A. Barrett
National Aeronautics and Space Administration
Lewis Research Center
Cleveland, Ohio 44135

SUMMARY

Seven alloying elements: Al, Cr, Ti, Nb, Ta, Mo, and W were added at two levels of concentration to produce a series of experimental nickel-base superalloys. Fifty alloys, representing a fraction of a 2^7 factorial design, were cast, tested, and analyzed. Each alloy's microstructure was characterized by phase extractions, x-ray diffraction, metallography and energy dispersive x-ray spectroscopy. Regression analysis was used to determine the effect of alloying element content on microstructure and stress-rupture life.

INTRODUCTION

The requirement for higher operating temperatures to produce increased efficiency in advanced gas turbines has lead to the development of complex nickel-base superalloys. Nickel-base superalloys are basically alloys of Ni with Cr and Al that also contain a few percent of some of the elements Ti, Nb, Ta, Mo, W, and Co as well as smaller amounts of C, B, Zr, and Hf. In gas turbine engines these materials are subjected to high stresses at high temperatures. Therefore, microstructural and morphological factors that affect stress-rupture life are important.

The work to be described was part of a study to obtain a better understanding of the effects of typical alloying elements in nickel-base superalloys on cyclic oxidation and hot corrosion. Fifty alloys, representing a statistically designed experiment, were prepared for testing. Concentrations of Cr, Al, Ti, Nb, Ta, Mo, and W in these alloys were systematically varied between two fixed levels.

The first portion of the study involved the evaluation of cyclic oxidation resistance at 1373 and 1423 K (ref. 1). Results of these tests showed that aluminum played the largest role in affecting oxidation. While boron was found to be very detrimental to oxidation resistance by allowing the formation of nickel oxide rather than protective alumina scales. The refractory metal effects were not so clear cut but the optimum oxidation resistant alloy was predicted by linear regression to be high Al (13 at. %), low Cr (10 at. %), low Ti (2 at. %), low Nb (1 at. %), and high Mo, W, and Ta (3 at. %) each.

Hot-corrosion testing of the alloys is reported in reference 2. Testing was conducted using a Mach 0.3 flame with 0.5 ppmw sodium at a temperature of 1173 K. Results showed the best corrosion resistance was achieved when the Cr content was greater than 14 at. %. However, some lower Cr-content alloys exhibited reasonable resistance provided that the Al and Ti contents were less than 5 at. % each. The effects of Nb, Ta, Mo, and W content on the hot-corrosion resistance varied depending on the Al and Ti content. At low Al

levels these elements appeared to be beneficial but as the Al content increases their effect becomes detrimental. These are preliminary results and a more complete statistical analysis will be the subject of a future publication.

The purpose of this study was to microstructurally characterize the alloys to obtain an initial assessment of the alloys' mechanical behavior.

APPROACH

Experimental Design

Seven alloying elements were varied at two levels spanning a portion of concentrations found in commercial nickel-base superalloys (table I). The elements, Cr and Al, were used to establish the corner points of the experimental design. Their composition levels were chosen from a plot of atomic percent Al versus atomic percent Cr for several commercial alloys (fig. 1). High and low levels were chosen to place two corner points inside and two corner points outside of the band formed by commercial alloys. For Al, the compositions selected were 13 and 5 at. %, and for Cr, 18 and 10 at. %. High and low levels chosen for the other elements were 6 and 2 at. % for Ti and 3 and 1 at. % for Nb, Ta, Mo, and W. Other elements commonly found in superalloys were intended to be held at fixed concentrations of: 10 Co, 0.5 C, 0.05 B, and 0.06 Zr, all in atomic percent.

A full 2^7 experimental design would consist of 128 alloys as shown in table II. A quarter replicate of the design was selected to limit the number of tests. The 32 alloys intended to form the quarter replicate experiment are shown in table II. An additional 18 alloys were added to the design in the high Al, low Cr region to provide more detail in the region of compositions nearest those of advanced cast superalloys. These additional alloys also increased the degrees of freedom for error estimates making it easier to judge the significance of the effects of the elements determined by regression analysis.

Alloy Preparation

The 50 alloys chosen from the experimental design were vacuum induction cast at 1755 K into an investment frame casting consisting of: 12 oxidation coupons, 8 tensile/stress rupture samples, and 4 hot-corrosion-burner-rig bars. Chemistry of each alloy was determined by spectrographic analysis and is tabulated in table III. It should be noted that three of the alloys, 7, 36, and 37, had high boron content. All tests were performed with the alloys in the as-cast condition. Stress rupture life was measured at 1023 K/600 MPa and 1273 K/100 MPa in air on duplicate samples from each alloy.

PHASE ANALYSIS AND MICROSTRUCTURE

Two phase extractions were performed on each of the alloys. The first, the carbide extraction, selectively allowed the collection of carbides, borides and topologically close-packed (TCP) phases, while the second, the gamma prime extraction, allowed the collection of gamma prime. Detailed procedures for

these extraction techniques can be found in the literature (refs. 3 to 6). Phases collected from each extraction were identified by x-ray diffraction using the Debye-Scherrer method (ref. 7). A computer program was used to calculate precise lattice parameters for the phases identified.

Metallographic and energy dispersive x-ray analysis were used to identify the morphology and elemental composition of the phases found by the previous phase extraction techniques.

REGRESSION ANALYSIS

The effects of composition on microstructure were modelled with the aid of regression analysis. Data were processed by standard statistical techniques, including stepwise regression (ref. 8) to fit the model:

$$w = B_0 + \sum_{i=1}^{7} B_i C_i \qquad (1)$$

where w is the estimated weight percentage of the phase, C is the atomic percentage of the element i, and the B's are the numerical coefficients to be determined by regression analysis. Only those alloys which contained some of the particular phase were used in developing the regression equation.

The effects of composition on stress-rupture life were also modelled with the aid of regression analysis. Data were processed by a computer program to fit the model:

$$\log t_r = B_0 + \sum_{i=1}^{11} B_i C_i + \sum_{i \neq j=1}^{7} B_{ij} (C_i - \bar{C}_i)(C_j - \bar{C}_j) \qquad (2)$$

where t_r is the time to rupture, C_i is the atomic percentage of the element i, $\bar{C}_i$ is the average C_i for all the alloys, and the B's are the numerical coefficients to be determined by regression analysis. The first summation includes the concentrations of Co, Zr, C, and B as well as those of the seven elements intentionally varied. However, for the interaction terms in the second summation, only the seven elements intentionally varied are considered. In the interaction terms the concentrations of the elements have been coded by subtracting the average value. This minimizes the correlation between the interaction terms and the terms for the two individual elements of which they consist (ref. 8).

The logarithm of t_r used as the dependent variable rather than t_r. It is expected that the error will be some fraction of t_r and increase with increasing t_r, rather than remain constant. Therefore by using $\log t_r$ the data with large t_r will not dominate the model.

Several alloys with high Al and Ti had zero lives. In regression analysis the actual form of the dependent variable used was $\log(t_r + 0.01)$. This was done to assign some finite life to the test so that $\log(t_r)$ could be used. The choice of 0.01 as the constant in $\log(t_r + 0.01)$ is purely arbitrary. Making the constant still closer to zero, 0.001 did not change the terms present in the model, the sign of any coefficients, or the goodness of fit to any

large degree. The fit using $\log(t_r + 0.01)$, while poor, was considerably better than that obtained using simply t_r as the dependent variable.

Stress rupture data were also fitted to a simple model of equation (2) with the interaction terms left out:

$$\log t_r = B_0 + \sum_{i=1}^{11} B_i C_i \qquad (3)$$

where the terms are discussed above for equation (2).

RESULTS

Typical microstructures of four alloys, one at each of the four corner points in the experimental design (fig. 1), are illustrated by optical micrographs in figure 2. Results show that large variations of microstructure were obtained for the composition levels chosen.

A summary of the phases identified in the carbide extraction residues by x-ray diffraction, is given in table IV. The presence of five phases (Laves, eta, sigma, tungsten and boride) varied with elemental content and are shown for each alloy in table V. All alloys contained γ, γ' and MC carbides, therefore these phases are not shown. The approximate concentrations of the phases are indicated by the size of the phase symbol. The three sizes of symbols indicate from smallest to largest, 0 to 10 at. %, 10 to 20 at. %, and 20 to 30 at. %. These rough estimates were obtained by subtracting 2 wt % from the carbide extraction residue to account for carbides. Then the remaining amount was proportioned to the diffracted x-ray intensity for each minor phases. Energy dispersive x-ray analysis results provided elemental composition of phases in situ. These results along with the x-ray diffraction results were used to identify the phases in the microstructure of each alloy. The morphology of the phases are shown in representative scanning electron micrographs in figure 3.

Laves, eta and sigma phases were each found in several alloys, with Laves being most common. The Laves phase identified was the $MgZn_2$ hexagonal $C14$ type which occurs in nickel-base alloys (refs. 9 to 12). Coefficients, calculated by regression analysis using equation (1), for the Laves phase are shown in table VI. The coefficients show Nb, Ta, W, Ti, and Al as promoting the formation of the Laves phase. In situ energy dispersive x-ray spectroscopy showed the Laves phase to contain Nb, Ta, Mo, W, Ni, Co, and Cr. The elements Nb and Ta contribute directly to the formation of the Laves phase, thus resulting in their positive contribution. The elements Al and Ti have a lesser indirect effect. Al and Ti appear to effectively tie up Ni by formation of the γ' phase, leaving the matrix more concentrated in the elements having low solubilities in γ', some of which contribute to Laves formation.

The coefficients of equation (1) for the amount of eta phase in the alloys are also shown in table VI. The coefficients show Ti and Mo have a positive contribution in forming the eta phase while Cr and Al have a negative contribution. In situ energy dispersive x-ray spectroscopy showed the eta phase to be comprised of Ni, Co, and Ti. The elements Ti and Mo are both predicted to significantly contribute to the amount of eta phase. The effect of Ti is expected

since Ni_3Ti is the prototype of the eta phase. The competing effect of Al is understood as stabilizing the Ni_3Al base γ' phase at the expense of the eta phase. The negative and positive contributions of Cr and Mo, respectively, to the formation of the eta phase are not understood and no explanation is offered.

The effects of the elements on the amount of sigma phase in the alloys cannot be explained by the simple model of the form used for Laves and eta. All of the elements except Al are rejected as having low probabilities of significance. When all the elements are kept in the equation only Mo and W are predicted to contribute to the formation of sigma. The value of R^2 adjusted for the number of degrees of freedom is only 30 percent. Energy dispersive x-ray spectroscopy could not be used to determine the elemental content of the believed sigma phase shown in figure 3(e) due to its small size.

The weight percent γ' extracted from each alloy is shown in table VII. Using equation (1), regression analysis of alloys containing only γ, γ', and MC carbides yields the coefficients shown in table VIII. These coefficients are used to calculate predicted values of weight percent γ', for all 50 alloys. The deviations from predicted values, i.e., predicted minus actual extracted values, are shown in parenthesis for each alloy in table VII. For alloys containing only γ, γ', and MC carbides the percent difference between actual and predicted weight percent γ' averaged less than 10 percent of the total. However, for alloys that contained TCP phases, the average difference was 100 percent and in the majority of alloys the predicted weight percent γ' was greater than the actual amount extracted. These large positive deviations from predicted values were due to the presence of TCP phases and the large-blocky morphology of the γ', both of which inhibited the complete extraction of γ'.

Examination of table VIII shows that the elements: Al, Nb, and Ta have a positive effect on the weight percent γ' in the alloys. These results are consistent with the others' findings that Al, Nb, and Ta partition to γ' (ref. 13). However, regression analysis shows the elements, Ta and Nb, are twice as potent as Al per at. % in increasing the weight percent γ'. The greater potency of Ta and Nb in increasing the weight percent γ' is believed to be associated with their greater atomic weights relative to Al, thus increasing the density of γ'. Energy dispersive x-ray spectroscopy analysis showed the presence of Ni, Cr, Nb, Ta, Al, and Ti in γ'. Why Ti is not significant in the regression analysis is not understood. Titanium is also known to partition to γ' (ref. 13), therefore a significant positive coefficient was expected.

Gamma prime lattice parameters are shown in table IX for each alloy. Results of regression analysis on the γ' lattice parameters using equation (1) are shown in table VIII. Again as in table IX the values in the parenthesis are the deviations from the predicted values which were calculated from the coefficients of table VIII.

The effect of each element on the lattice parameter of γ' can be understood by the element's percent difference in atomic diameter from nickel versus the percent difference in atomic diameter from nickel for the element it substitutes for in γ'. Aluminum has a +6 percent difference in atomic diameter from Ni (ref. 13). Titanium and Ta substitute for Al in γ' and have differences of +9 and 18 percent in atomic diameter from Ni, respectively. This

could explain Ti and Ta's positive effect in increasing γ' lattice parameter. Chromium can substitute for Ni in γ' and has a +3 percent difference in atomic diameter from Ni, hence it also has a positive effect on the lattice parameter of γ'. The negative coefficient for Al is due to it being the element with the lowest percentage increase in atomic diameter from Ni that partitions to γ'.

Stress rupture life and percent elongation for each alloy are shown in table X for 1023 K/600 MPa and table XI for 1273 K/100 MPa. The coefficients of the significant terms in the models for 1023 K/600 MPa and 1273 K/100 MPa stress rupture tests are shown in table XII together with the values of R^2, R^2 adjusted for the number of degrees of freedom, and the standard deviation of the dependent variable around the regression line. These equations are lengthy and difficult to relate to the data shown in tables X and XI, primarily because of the interactive effects of the elements. However, simple models (table XIII) without interaction terms yield poor fits, with R^2 of 60 to 65 percent, and actually predicted opposite effects of a few elements from those predicted by the full model. Plots of predicted versus observed values of $\log t_r$ from the models are shown in figures 4 and 5 for the 1023 K/600 MPa and 1273 K/100 MPa test, respectively.

DISCUSSION

The microstructures varied significantly over the range of Cr and Al concentrations selected. Thirty-six of the alloys contained topologically-close-packed (TCP) phases. The occurrence of the TCP phases can be related to the atomic percent of Ni + Co contained in each alloy (ref. 14). The Ni + Co level for 31 of the 36 alloys containing TCP phases (table III) was less than 70 atomic percent. The remaining five alloys had high levels of Ti and formed the eta phase Ni_3Ti.

Four of the 14 alloys that did not contain TCP phases, alloys 10, 36, 37, and 38, had Ni + Co levels less than 70 atomic percent. The absence of TCP phases in these alloys can be explained. Alloys 10 and 38 had low levels of Nb, Ta, W, and Mo, therefore the concentration of elements that form TCP phases did not saturate in the matrix. Alloys 36 and 37 had high boron contamination which caused the formation of borides, $(CrMoW)_3B_2$, removing elements from the matrix which form TCP phases.

Regression analysis of the stress rupture data showed that even with the interaction terms included in the model, the degree of fit is not high, especially for the 1023 K/600 MPa tests. It is difficult to express the life of the 1023 K/600 MPa test as a function of composition, since in some regions of composition life is zero and independent of composition. Furthermore, the models are not valid for compositions outside the range of the present experiment. For instance, the model for 1023 K/600 MPa stress-rupture life predicts that if all the Al were removed from the alloy representing the average composition, life would increase by a factor of about three. The interaction terms would all be zero since the concentration of the second element would equal its average, and since B_{Al} is negative, less Al would mean a more positive $\log t_r$.

It is believed that the influence of casting inhomogeneities contributed to the poor fit with stress-rupture life. This could especially be the case

for the alloys in this experiment because of their high alloy content. Evidence of inhomogeneities was seen in a few of the high-tungsten-content alloys which exhibited a tungsten phase (fig. 3(b)) believed to be due to insufficient melting. Inhomogeneities most likely existed in other alloys but it was beyond the scope of this experiment to include this factor.

If we restrict our consideration to the composition range of the experiment we can obtain some understanding of the effects the individual elements have on stress-rupture life. Consider changes from the average composition. Generally, for both tests the coefficients of the individual element terms and those of the interaction terms are negative. This can be understood by the realization that the average composition is so highly alloyed that increasing the concentration of almost any of the alloying elements will decrease life unless, as expressed by the negative coefficients of the interaction terms, the concentration of some of the other alloying elements are reduced. This result implies that the occurrence of TCP phases reduces stress-rupture life.

It may be seen that in the models for both tests, Al has only a small negative direct effect, and because of its negative interactions with Ti, Nb, Ta and Mo, stress-rupture life should increase with increasing Al if the other elements are decreased. This may be seen clearly in the data for the 1273 K/100 MPa test (table XI). The best alloys appear in the region of the high Al, low Ti, low Ta and low Nb. The exception to this generalization is alloy 37, which has high Al, low Ti, low Ta, but high Nb. This result is due to an accidentally high boron concentration in Alloy 37 which is quite beneficial as reflected by the positive coefficient in the model (table XII). For the 1023 K/600 MPa test it is not so clear where the best alloys lie. Several alloys in the high Al, low Ti, and low Cr region of table X have reasonable lives. Again Alloy 37 stands out with a very long life, but overall in this data set the probability of significance of the boron effect was low and the term was rejected.

In analyzing both the stress-rupture and oxidation data, an optimum alloy is predicted by regression analysis at high Al (13 at. %), low Cr (10 at. %), low Ti (2 at. %), low Nb (1 at. %), and high Mo, W, and Ta (3 at. %) each. Although boron was not intentionally varied it was interesting to note its apparent positive effect on stress-rupture life while drastically reducing oxidation resistance.

Preliminary analysis of the hot-corrosion data showed that high Cr and low Al contents increased corrosion resistance. This is in direct conflict with the results of stress-rupture life and oxidation resistance which were optimized at low Cr and high Al contents. A complete statistical analysis of stress-rupture life, cyclic oxidation, and hot-corrosion resistance will be the subject of a future publication.

SUMMARY

The effects of seven alloying elements on microstructure and stress-rupture life of nickel-base superalloys were studied using a statistically designed experiment. Fifty alloys, representing a partial fraction of a 2^7 factorial design, were produced and examined. Regression equations were calculated to show the effect of each element on; presence of minor phases, weight percent γ, γ' lattice parameter and stress rupture life. Regression analysis results showed that:

(1) Laves phase was promoted by Nb, Ta, Ti and Al.

(2) Eta phase was promoted by Mo and Ti.

(3) Weight percent γ' increased with increasing Al, Ta, and Nb.

(4) The γ' lattice parameter increased with increasing Ti, Ta, and Cr; and decreased with increasing Al.

(5) Stress rupture properties decreased with increasing concentration of Al, Cr, Ti, Nb, Ta, Mo, and W for the composition range studied.

(6) An alloy with optimum stress-rupture and cyclic oxidation resistance is predicted at high Al (13 at. %), low Cr (10 at. %), low Ti (2 at. %), low Nb (1 at. %), and high Mo, W, and Ta (3 at. %) each.

REFERENCES

1. Barrett, C. A.; Miner, R. V.; and Hull, D. R.: The Effects of Cr, Al, Ti, Mo, W, Ta, and Cb on the Cyclic Oxidation Behavior of Cast Ni-Base Superalloys at 1100 and 1150 C. Oxid. Met., vol. 20., nos. 5/6, Dec. 1983, pp. 255-278.

2. Deadmore, Daniel L.: Effects of Alloy Composition on Cyclic Flame Hot-Corrosion Attack of Cast Nickel-Base Superalloys at 900° C. NASA TP-2338, 1984.

3. Donachie, M. J., Jr.; and Kriege, O. H.: Phase Extraction and Analysis in Superalloys-Summary of Investigations by ASTM Committee E-4 Task Group 1. J. Mater., vol. 7, no. 3, Sept. 1972, pp. 269-278.

4. Donachie, M. J., Jr.: Phase Extraction and Analysis in Superalloys-Second Summary of Investigations by ASTM Subcommittee E04.91. J. Test. Eval., vol. 6, no. 3, May 1978, pp. 189-195.

5 Kriege, O. H.: Phase Seperation as a Technique for the Characterization of Superalloys. Metallography-A Practical Tool for Correlating the Structure and Properties of Materials. ASTM STP 557, American Society for Testing and Materials, 1974, pp. 220-234.

6 Kriege, Owen H.; and Baris, J. M.: The Chemical Partitioning of Elements in Gamma Prime Separated from Precipitation-Hardened, High-Temperature Nickel-Base Alloys. ASM Trans. Q., vol. 62, no. 1, Mar. 1969, pp. 195-200.

7. Cullity, Bernard Dennis: Elements of X-ray Diffraction. Second Ed. Addison-Wesley Publishing Co., Inc., 1978, pp. 161-168.

8. Montgomery, Douglas C.; and Peck, Elizabeth A.: Introduction to Linear Regression Analysis. John Wiley and Sons, 1982.

9. Johannes, R. L.; Haydock, R.; and Heine, Volker: Phase Stability in Transition-Metal Laves Phases. Phys. Rev. Lett., vol. 36, no. 7, Feb. 16, 1976, pp. 372-376.

10. Sabol, G. P.; and Stickler, R.: Microstructure of Nickel-Based Superalloys. Phys. Status Solidi, vol. 35, no. 1, Sept. 1, 1969, pp. 11-51.

11. Berry, R. L.; and Raynor, G. V.: The Crystal Chemistry of the Laves Phases. Acta Crystallogr., vol. 6, 1953, pp. 178-186.

12. Edwards, A. R.: The Lattice Dimensions of the AB_2 Laves Phases. Metall. Trans., vol. 3, no. 6, June 1972, pp. 1365-1372.

13. Decker, R. F.: Strengthening Mechanisms in Nickel-Base Superalloys. The International Nickel Company.

14. Dreshfield, R. L.: Estimation of Conjugate γ and γ' Compositions in Ni-Base Superalloys. Applications of Phase Diagrams in Metallurgy and Ceramics, G. C. Carter, ed. NBS-SP-496-VOL-1, National Bureau of Standards, 1978, pp. 624-659.

TABLE I. - HIGH AND LOW LEVELS OF ELEMENTS INTENTIONALLY VARIED

Element	Atomic percent	
	High	Low
Cr	18	10
Al	13	5
Ti	6	2
Ta	3	1
Nb	3	1
W	3	1
Mo	3	1

Balance Ni with 10 Co,
0.1 C, 0.01 B and
0.1 Zr.

TABLE II. - 2^7 FACTORIAL EXPERIMENTAL DESIGN

Ti, at. %	Nb, at. %	Cr, at. %	W, at. %	Mo, at. %	5 at. % Al		13 at. % Al	
					1 at. % Ta	3 at. % Ta	1 at. % Ta	3 at. % Ta
6	3	18	3	3		[b]7		
				1			[b]17	
			1	3			[b]18	
				1		[b]8		
		10	3	3				[b]39
				1	[a]27		45	
			1	3	[b]28		47	
				1	29		49	[b]42
	1	18	3	3	[b]9			
				1				[b]15
			1	3				[b]16
				1	[b]10			
		10	3	3			[b]44	
				1		[b]25	46	40
			1	3		[b]26	48	41
				1			[b]50	43
2	3	18	3	3				[b]11
				1				
			1	3	[b]5			
				1	4,6			[b]12
		10	3	3		[b]19		
				1			[b]33	
			1	3			[b]35	
				1		[b]20	37	
	1	18	3	3			[b]13	
				1		[b]1		
			1	3		[b]2		
				1		3	[b]14	
		10	3	3	[b]22			
				1	23		34	[b]30
			1	3			36	[b]31
				1	[b]24	21	38	32

[a]Number refers to alloy designation given in table III.
[b]Alloys of quarter replicate design.

TABLE III. - CHEMISTRY OF 50 ALLOYS IN 2^7 EXPERIMENTAL DESIGN IN ATOMIC PERCENT

Alloy	Element												
	Cr	Al	Ti	Nb	Ta	W	Mo	Co	B	C	Zr	Ni	Ni+Co
1	16.73	5.13	1.65	0.86	2.40	3.13	0.78	9.20	0.06	0.37	0.05	59.61	[a]68.81
2	15.46	4.84	1.60	.98	2.37	1.04	2.62	9.32	.06	.31	.05	61.36	70.68
3	15.53	5.09	1.80	.95	2.45	1.01	.92	9.32	.06	.15	.01	62.72	72.04
4	16.96	4.84	1.85	2.80	1.02	.98	.96	9.45	.06	.15	.05	60.89	70.34
5	16.68	4.67	1.79	2.90	0.99	.99	2.75	9.32	.06	.35	.07	59.44	[a]68.76
6	16.35	4.85	1.91	2.83	.94	.99	.97	9.42	.06	.30	.06	61.32	70.74
7	15.80	5.26	4.03	2.34	1.94	3.42	2.45	8.95	.58	3.11	.06	52.07	[a]61.02
8	14.08	4.85	5.08	2.70	2.36	1.03	.86	9.11	.06	.51	.06	59.34	[a]68.45
9	16.55	5.19	5.52	1.02	.90	3.12	2.53	9.13	.11	.36	.05	55.53	[a]64.66
10	15.60	4.97	6.05	1.11	.97	1.20	1.01	9.18	.05	.25	.06	59.60	68.78
11	15.67	14.85	1.73	2.45	2.14	2.81	2.37	8.95	.11	.45	.01	48.47	[a]57.42
12	14.64	14.75	1.64	2.54	2.30	1.45	.93	8.99	.05	.39	.05	52.28	[a]61.27
13	17.08	15.68	1.63	.94	.90	3.39	2.48	9.01	.11	.34	.04	48.39	[a]57.40
14	16.76	14.35	2.02	1.06	.93	1.00	.97	9.15	.05	.19	.06	53.48	[a]62.63
15	15.26	15.53	4.93	1.14	2.01	2.86	.80	8.98	.11	.34	.05	47.99	[a]56.97
16	14.08	14.92	5.16	.95	2.25	1.35	2.72	8.83	.05	.34	.04	49.30	[a]58.13
17	16.09	15.06	5.69	2.64	.82	2.69	.90	8.97	.05	.34	.06	46.70	[a]55.67
18	14.46	15.08	5.70	2.32	.83	1.22	2.93	8.92	.05	.52	.06	47.92	[a]56.84
19	10.08	7.79	1.67	2.53	2.51	3.14	2.42	9.73	.12	.43	.04	59.55	[a]69.28
20	9.22	5.08	1.72	2.60	2.61	1.30	.94	9.96	.06	.26	.04	66.22	[a]76.18
21	9.49	5.35	1.79	1.04	3.07	.98	.86	10.05	.06	.36	.06	66.89	76.95
22	8.73	5.02	1.66	.94	1.05	2.76	2.57	9.93	.12	.20	.06	66.90	76.73
23	9.36	4.48	1.87	.95	1.03	2.69	.90	9.84	.06	.31	.05	68.49	78.33
24	10.52	4.34	2.02	.99	1.05	.94	.92	10.05	.06	.30	.05	68.76	78.81
25	8.03	4.92	4.99	.91	2.86	2.60	.84	9.65	.12	.42	.06	64.59	[a]74.24
26	8.36	4.90	5.03	.95	3.00	1.01	2.61	9.65	.06	.41	.05	63.95	[a]73.60
27	8.19	4.94	5.08	2.68	.98	2.73	.92	9.60	.06	.46	.06	64.31	[a]73.91
28	9.78	4.87	5.33	2.93	.99	.76	2.73	9.76	.06	.35	.13	63.32	[a]73.08
29	9.48	4.73	5.86	2.19	1.02	1.00	.98	9.07	.06	.30	.06	65.26	74.33
30	8.58	13.25	1.83	.98	2.91	2.63	.87	9.72	.11	.20	.06	58.86	[a]68.58
31	8.61	12.46	1.73	.98	2.94	1.34	2.55	9.77	.06	.20	.06	59.30	[a]69.07
32	9.20	13.22	1.86	1.00	2.93	1.00	.90	9.73	.06	.39	.06	59.66	[a]69.39
33	8.81	13.29	1.69	2.69	.97	2.77	.89	9.68	.11	.30	.06	58.76	[a]68.44
34	8.95	13.31	1.81	.91	.94	2.78	.88	9.74	.11	.20	.10	60.28	70.02
35	9.36	13.16	1.83	2.58	.94	1.05	2.81	9.62	.05	.43	.07	57.91	[a]67.73
36	9.61	12.76	1.84	1.06	.98	1.05	2.84	9.58	1.58	.47	.06	58.18	67.76
37	9.56	12.23	1.87	2.68	1.01	1.03	.98	9.63	1.05	.95	.07	58.99	68.62
38	10.14	14.47	2.32	1.02	.85	1.07	.95	9.66	.05	.37	.08	59.01	68.67
39	7.18	12.56	4.88	2.52	2.69	2.36	2.16	9.70	.06	.61	.05	54.80	[a]64.50
40	8.04	13.64	5.32	.97	2.71	2.91	.82	9.63	.06	.56	.07	55.30	[a]64.93
41	7.77	14.02	5.05	.94	2.69	1.40	2.56	9.53	.06	.25	.07	55.68	[a]65.21
42	7.35	13.43	5.10	2.48	2.84	1.33	.94	9.55	.06	.10	.05	56.77	[a]66.32
43	7.90	13.55	5.26	.95	2.79	1.14	.91	9.56	.05	.24	.04	57.60	[a]67.16
44	8.49	14.10	5.13	.96	1.02	2.09	2.51	9.59	.05	.39	.06	55.67	[a]65.22
45	8.26	12.01	5.54	2.70	1.06	3.39	.98	9.77	.06	.25	.05	55.93	[a]65.70
46	8.96	13.80	5.42	1.07	.91	2.17	.95	9.58	.05	.34	.06	56.70	[a]66.28
47	8.75	13.57	5.31	2.80	.87	1.13	2.85	9.54	.05	.38	.06	54.69	[a]64.23
48	9.13	10.73	5.41	1.08	.94	1.08	2.89	9.70	.05	.43	.06	58.49	[a]68.19
49	8.46	13.50	5.65	2.86	.97	1.15	.96	9.58	.05	.29	.07	56.50	[a]66.08
50	9.61	13.43	5.73	1.05	.90	1.05	1.04	9.55	.05	.42	.06	57.11	[a]66.66

[a]Alloys containing topologically-close-packed phases.

TABLE I" - SUMMARY OF PHASES IDENTIFIED BY X-RAY DIFFRACTION

Phase	Crystal structure	Lattice parameter(s), nm	Type	Elemental content[a]
Boride	Tetragonal	a = 0.581 c = 0.314	M_3B_2	Cr, Mo, W
Carbide	Face-centered-cubic	a = 0.437-0.446	MC	Ti, Ta, Nb
Eta	Hexagonal	a = 0.51 c = 0.83	A_3B	Ni, Ti
γ'	Ordered face-centered-cubic	a = 0.3586-0.3604	A_3B	Ni, Al, Ti
Laves	Hexagonal	a = 0.478 c = 0.78	AB_2	Cr, Ni, Co, Ta, Nb, Mo, W
Sigma	Tetragonal	a = 0.89 c = 0.46	----	----------
Tungsten	Body-centered-cubic	a = 0.314	M	W, Cr

[a]Elemental content determined by EDXS.

TABLE V. - PHASES IDENTIFIED IN EACH ALLOY BY X-RAY DIFFRACTION OF EXTRACTION RESIDUES

					5 at. % Al		13 at. % Al	
Ti, at. %	Nb, at. %	Cr, at. %	W, at. %	Mo, at. %	1 at. % Ta	3 at. % Ta	1 at. % Ta	3 at. % Ta
6	3	18	3	3		7 L$_t$		
				1			17 LW	
			1	3			18 L	
				1		8 L$_\eta$		
		10	3	3				39 LW
				1	27 L$_\eta$B		45 L$_\sigma$W	
			1	3	28 L$_\eta$		47 L$_\sigma$	
				1	29		49 L$_\sigma$	42 L
	1	18	3	3	9 L$_\sigma$W			
				1				15 L
			1	3				16 L
				1	10			
		10	3	3			44 L$_\sigma$W	
				1		25 $_\eta$	46 L$_\sigma$W	40 L$_\sigma$W
			1	3		26 $_\eta$	48 L$_\sigma$	41 L$_\sigma$
				1			50 L$_\sigma$	43 L
2	3	18	3	?				11 LW
				1				
			1	3	5 L			
				1	4,6			12 L
		10	3	3		19 LW		
				1			33 L	
			1	3			35 L	
				1		20 $_\eta$	37 B	
	1	18	3	3			13 L$_\sigma$W	
				1		1 L		
			1	3		2		
				1		3	14 L$_\sigma$	
		10	3	3	22			
				1	23		34	30 L$_\sigma$W
			1	3			36 B	31 L$_\sigma$
				1	24	21	38	32 L$_\sigma$

[a]Phases present in alloy. (L = Laves, $_\eta$ = eta, $_\sigma$ = sigma, B = Boride, W = Tungsten). Phase symbol size represents amount of phase in weight percent. 0 to 10; L, 10 to 20; L, 20 to 30; L.

TABLE VI. - COEFFICIENTS OF SIGNIFICANT TERMS
IN EQUATION (1) FOR THE LAVES AND ETA PHASES

Term	Laves		Eta	
	Coefficient	T-ratio	Coefficient	T-ratio
B_o	-28.7	-5.7	13.2	2.9
Al	1.20	5.9	-1.09	-3.1
Ti	1.58	3.6	2.12	3.0
Nb	4.71	4.9		
Ta	4.09	4.3		
Mo			2.13	2.1
W	2.10	2.6		
Cr			-1.19	-5.1
	R^2 = 71.5 R^2 adj = 66.2 s = 4.2 v = 33-6 = 27		R^2 = 87.4 R^2 adj = 77.4 s = 2.4 v = 10-5 = 5	

TABLE VII. - WEIGHT PERCENT OF GAMMA PRIME EXTRACTED FROM EACH ALLOY

					5 at. % Al		13 at. % Al	
Ti, at. %	Nb, at. %	Cr, at. %	W, at. %	Mo, at. %	1 at. % Ta	3 at. % Ta	1 at. % Ta	3 at. % Ta
6	3	18	3	3		7 48.0(-1.9)		
				1			17 21.0(+54.7)	
			1	3			18 21.0(+52.7)	
				1		8 35.1(+14.9)		
		10	3	3				39 61.9(+18.9)
				1	[a]27 35.7(+4.5)	45 56.0(+10.7)		
			1	3	28 37.3(+4.4)		47 23.2(+48.4)	
				1	29 36.7(-0.3)		49 31.1(+41.5)	42 58.7(+24.7)
	1	18	3	3	9 43.7(-14.2)			
				1				15 13.0(+63.1)
			1	3				16 7.3(+67.1)
				1	10 38.7(-9.1)			
		10	3	3			44 32.4(+30.1)	
				1		25 36.0(+6.2)	46 37.9(+23.4)	40 50.1(+23.1)
			1	3		26 34.4(+8.8)	48 50.7(-0.3)	41 33.4(+40.8)
				1			50 42.1(+17.3)	43 4[illegible].3(+28.0)
2	3	18	3	3				11 30.9(+52.3)
				1				
			1	3	5 38.1(+2.6)			
				1	4,6 37.4(+3.2)			12 36.1(+48.6)
		10	3	3		19 56.0(+4.8)		
				1			33 43.5(+27.2)	
			1	3			35 46.9(+22.3)	
				1		20 55.5(-3.5)	37 68.3(-1.3)	
	1	18	3	3			13 40.8(+26.5)	
				1		1 43.0(-3.8)		
			1	3		2 41.0(-2.4)		
				1		3 41.6(-1.7)	14 55.0(+8.4)	
		10	3	3	22 28.5(+0.9)			
				1	23 23.1(+4.1)		34 60.7(-2.0)	30 39.3(+34.0)
			1	3			36 60.9(-2.9)	31 44.1(+26.5)
				1	24 22.5(+4.8)	21 38.4(+7.6)	38 66.9(-3.9)	32 69.1(+ 4.3)

[a]Values in parenthesis are predicted minus actual amounts extracted.

TABLE VIII. - COEFFICIENTS OF SIGNIFICANT TERMS IN EQUATION (1) FOR WEIGHT PERCENT GAMMA PRIME EXTRACTED AND GAMMA PRIME LATTICE PARAMETERS

Term	Weight percent, γ' in alloy		Lattice parameter of γ' in alloy, nm	
	Coefficient	T-ratio	Coefficient	T-ratio
B_0	-2.7	-0.5	0.3582	1268
Al	3.65	10.0	-.0000635	-4.7
Ti	-----	----	.0000928	2.5
Nb	6.65	3.6	---------	------
Ta	7.26	3.8	.0003950	5.4
Mo	-----	----	---------	------
W	-----	----	---------	------
Cr	-----	----	.0000769	5.5
	R^2 = 89.9 R^2_{adj} = 87.4 s = 5.2 v = 16 - 4 = 12		R^2 = 94.0 R^2_{adj} = 91.8 s = 0.00018 v = 16 - 5 = 11	

TABLE IX. - LATTICE PARAMETERS OF GAMMA PRIME IN NANOMETERS

Ti, at. %	Ni, at. %	Cr, at. %	W, at. %	Mo, at. %	5 at. % Al		13 at. % Al	
					1 at. % Ta	3 at. % Ta	1 at. % Ta	3 at. % Ta
6	3	18	3	3		7 0.3602(+1)		
				1			17 0.3600(-6)	
			1	3			18 .3602(-10)	
				1		8 .3606(-10)		
		10	3	3				35 0.3604(-9)
				1	[a]27 0.3600(-6)		45 .3598(-8)	
			1	3	28 .3599(-4)		47 .3595(-6)	
				1	29 .3597(-1)		49 .3599(-10)	42 .3603(-7)
	1	18	3	3	9 .3600(+1)			
				1				15 .3599(-2)
			1	3				16 .3598(-1)
				1	10 .3600(+1)			
		10	3	3			44 .3594(-5)	
				1		25 .3602(-1)	46 .3593(-4)	40 .3599(-3)
			1	3		26 .3600(+2)	48 .3592(-1)	41 .3604(-9)
				1			50 .3593(-3)	43 .3599(-3)
2	3	18	3	3				11 .3602(0)
				1				
			1	3	5 .3602(-4)			
				1	4,6 .3600(-3)			12 .3601(-7)
		10	3	3		19 .3604(-7)		
				1			33 .3593(+1)	
			1	3			35 .3593(-6)	
				1		20 .3600(-2)	37 .3589(-1)	
	1	18	3	3			13 .3592(0)	
				1		1 .3604(-1)		
			1	3		2 .3602(0)		
				1		3 .3603(-1)	14 .3590(+2)	
		10	3	3	22 .3589(+3)			
				1	23 .3593(0)		34 .3589(-3)	30 .3591(+3)
			1	3			36 .3586(+1)	31 .3592(+2)
				1	24 .3593(+1)	21 .3586(+2)	38 .3586(+1)	32 .3593(+1)

[a]Values in parenthesis are (predicted minus observed) x 10^4.

TABLE X. - STRESS RUPTURE LIFE IN HOURS MEASURED AT 1023 K/600 MPa

Ti, at. %	Nb, at. %	Cr, at. %	W, at. %	Mo, at. %	5 at. % Al		13 at. % Al	
					1 at. % Ta	3 at. % Ta	1 at. % Ta	3 at. % Ta
6	3	18	3	3		7 0.0(0.0)		
				1			17 0.0(0.0)	
			1	3			18 .0(0.0)	
				1		8 .2(0.8)		
		10	3	3				39 0.0(0.0)
				1	[a]27 11.7(0.8)		45 .0(0.0)	
			1	3	28 0.8(0.4)		47 .0(0.0)	
				1	29 .4(2.1)		49 .0(0.4)	42 .0(0.4)
	1	18	3	3	9 .1(0.0)			
				1				15 .0(0.0)
			1	3				16 .0(1.4)
				1	10 8.1(1.2)			
		10	3	3			44 35.3(4.4)	
				1		25 2.6(2.0)	46 51.1(2.0)	40 .0(1.6)
			1	3		26 6.1(1.3)	48 83.9(3.2)	41 .0(0.0)
				1			50 68.5(4.8)	43 .0(0.0)
2	3	18	3	3				11 NO TEST
				1				
			1	3	5 11.8(4.8)			
				1	4,6 29.8(3.3)			12 .0(0.0)
		10	3	3		19 15.1(0.8)		
				1			33 211.7(6.0)	
			1	3			35 110.0(8.4)	
				1		20 8.5(1.6)	37 951.0(4.9)	
	1	18	3	3			13 .0(0.0)	
				1		1 7.1(1.6)		
			1	3		2 56.4(4.0)		
				1		3 73.1(4.4)	14 21.6(2.5)	
		10	3	3	22 1.3(3.6)			
				1	23 .0(2.8)		34 13.3(0.4)	30 224.4(7.2)
			1	3			36 140.4(0.4)	31 131.1(4.0)
				1	24 .0(0.9)	21 10.8(1.6)	38 120.4(2.1)	32 250.2(5.5)

[a]Values in parenthesis are percent elongation.

TABLE XI. - STRESS RUPTURE LIFE IN HOURS MEASURED AT 1273 K/100 MPa

					5 at. % Al		13 at. % Al	
Ti, at. %	Nb, at. %	Cr, at. %	W, at. %	Mo, at. %	1 at. % Ta	3 at. % Ta	1 at. % Ta	3 at. % Ta
6	3	18	3	3		7 6.0(13.6)		
				1			17 0.9(44.2)	
			1	3			18 2.8(56.0)	
				1		8 5.1(14.2)		
		10	3	3				39 1.9(10.2)
				1	[a]27 19.4(14.6)		45 4.8(14.0)	
			1	3	28 7.3(13.7)		47 4.5(17.8)	
				1	29 8.9(14.8)		49 2.8(17.7)	42 2.0(1.0)
	1	18	3	3	9 11.2(22.7)			
				1				15 1.2(48.2)
			1	3				16 0.4(65.5)
				1	10 19.4(10.6)			
		10	3	3			44 10.0(19.3)	
				1		25 51.4(10.3)	46 11.7(6.2)	40 3.2(13.6)
			1	3		26 36.1(6.7)	48 49.6(2.5)	41 2.2(14.6)
				1			50 23.1(9.8)	43 5.4(12.8)
2	3	18	3	3				11 2.2(23.3)
				1				
			1	3	5 14.8(13.0)			
				1	4,6 18.6(19.9)			12 2.8(29.8)
		10	3	3		19 35.0(13.4)		
				1			33 129.2(5.1)	
			1	3			35 83.8(4.5)	
				1		20 16.4(16.3)	37 476.2(11.0)	
	1	18	3	3			13 6.0(16.8)	
				1		1 23.0(8.2)		
			1	3		2 35.2(11.0)		
				1		3 21.8(4.4)	14 16.2(6.8)	
		10	3	3	22 43.0(25.6)			
				1	23 14.0(31.4)		34 303.3(4.0)	30 15[illegible].0(6.3)
			1	3			36 344.8(4.8)	31 160.1(6.2)
				1	24 1.8(45.5)	21 70.0(11.3)	38 264.6(4.8)	32 154.0(4.0)

[a]Values in parenthesis are percent elongation.

TABLE XII. - COEFFICIENTS OF SIGNIFICANT TERMS FOR THE FULL MODEL ON STRESS RUPTURE DATA

Term	Mean composition C_i, at%	1023 K/600 MPa		1273 K/100 MPa	
		Coefficient	T-ratio	Coefficient	T-ratio
B_0	------	6.64	9.59	4.7357	14.94
Al	10.166	-0.0565	-2.39	-0.0199	-2.98
Ti	3.568	-.5020	-8.92	-.2057	-16.21
Nb	1.703	-.5771	-4.81	-.1996	-5.75
Ta	1.634	-.5514	-4.53	-.2908	-6.90
Mo	1.599	-------	-----	-.0912	-2.71
W	1.799	-.2507	-2.21	-.0823	-2.45
Cr	11.325	-.1625	-5.12	-.0954	-10.13
Co	9.478	-------	-----	-------	------
Zr	.058	-------	-----	-5.863	-2.28
B	.125	-------	-----	.3687	3.03
C	.352	-------	-----	-------	------
AlTi	------	-.0543	-4.15	-.0350	-8.80
AlNb	------	-.0877	-3.12	-.0409	-4.40
AlTa	------	-.1599	-5.47	-.0695	-8.11
AlMo	------	-.0599	-2.19	-.0333	-4.09
AlW	------	-------	-----	-.0219	-2.86
AlCr	------	-.0276	-4.05	-.0158	-8.77
TiNb	------	-.2866	-4.11	-------	------
TiTa	------	-.3898	-5.75	-.0917	-4.45
TiMo	------	-------	-----	-------	------
TiW	------	-------	-----	-.0394	-2.07
TiCr	------	-------	-----	-.0167	3.26
NbTa	------	-------	-----	-.1157	-2.19
NbMo	------	-------	-----	-------	------
NbW	------	-------	-----	-------	------
NbCr	------	-------	-----	-------	------
TaMo	------	-------	-----	-------	------
TaW	------	-------	-----	-------	------
TaCr	------	-------	-----	-.0445	-3.56
MoW	------	-------	-----	-.1793	-3.44
MoCr	------	-.0792	-2.26	-------	------
WCr	------	-.0708	-2.21	-------	------
		R^2 = 77.6 R^2_{adj} = 73.2		R^2 = 89.8 R^2_{adj} = 87.2	

TABLE XIII. - COEFFICIENTS OF SIGNIFICANT TERMS FOR THE SIMPLE MODEL ON STRESS RUPTURE DATA

Term	1023 K/600 MPa		1273 K/100 MPa	
	Coefficient	T-ratio	Coefficient	T-ratio
B_0	-0.4053	-0.85	2.4557	7.32
Al	.2058	9.72	-0.0231	-2.04
Ti	--------	-----	-.2426	-8.50
Nb	.2942	2.75	-.1815	-3.05
Ta	.3224	3.07	-------	-----
Mo	--------	-----	-------	-----
W	-.2424	-2.60	-------	-----
Cr	--------	-----	-.0595	-3.90
Co	--------	-----	-------	-----
Zr	-11.671	-2.46	12.426	4.03
B	--------	-----	.6742	3.51
C	--------	-----	-------	-----
	R^2 = 64.9		R^2 = 60.2	
	R^2_{adj} = 61.8		R^2_{adj} = 57.7	

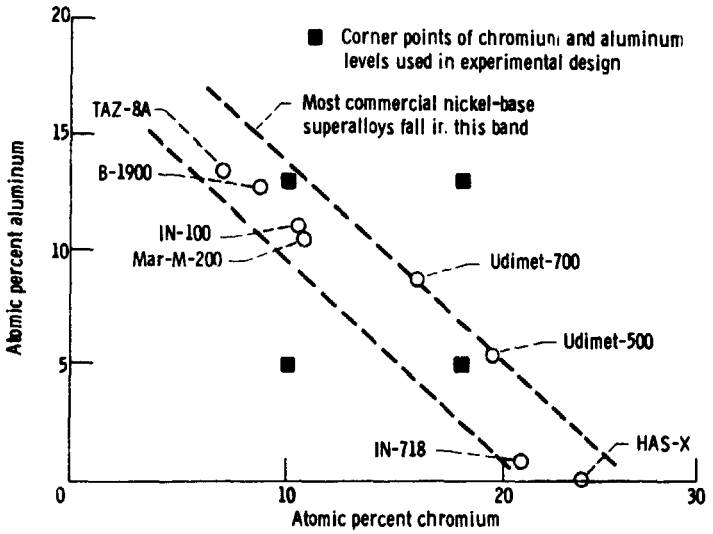

Figure 1. - Atomic percent chromium versus aluminum for several commercial nickel-base superalloys. Experimental design spans a range of concentrations based on corner points at high and low levels of 18 and 10 percent chromium and 13 and 5 percent aluminum.

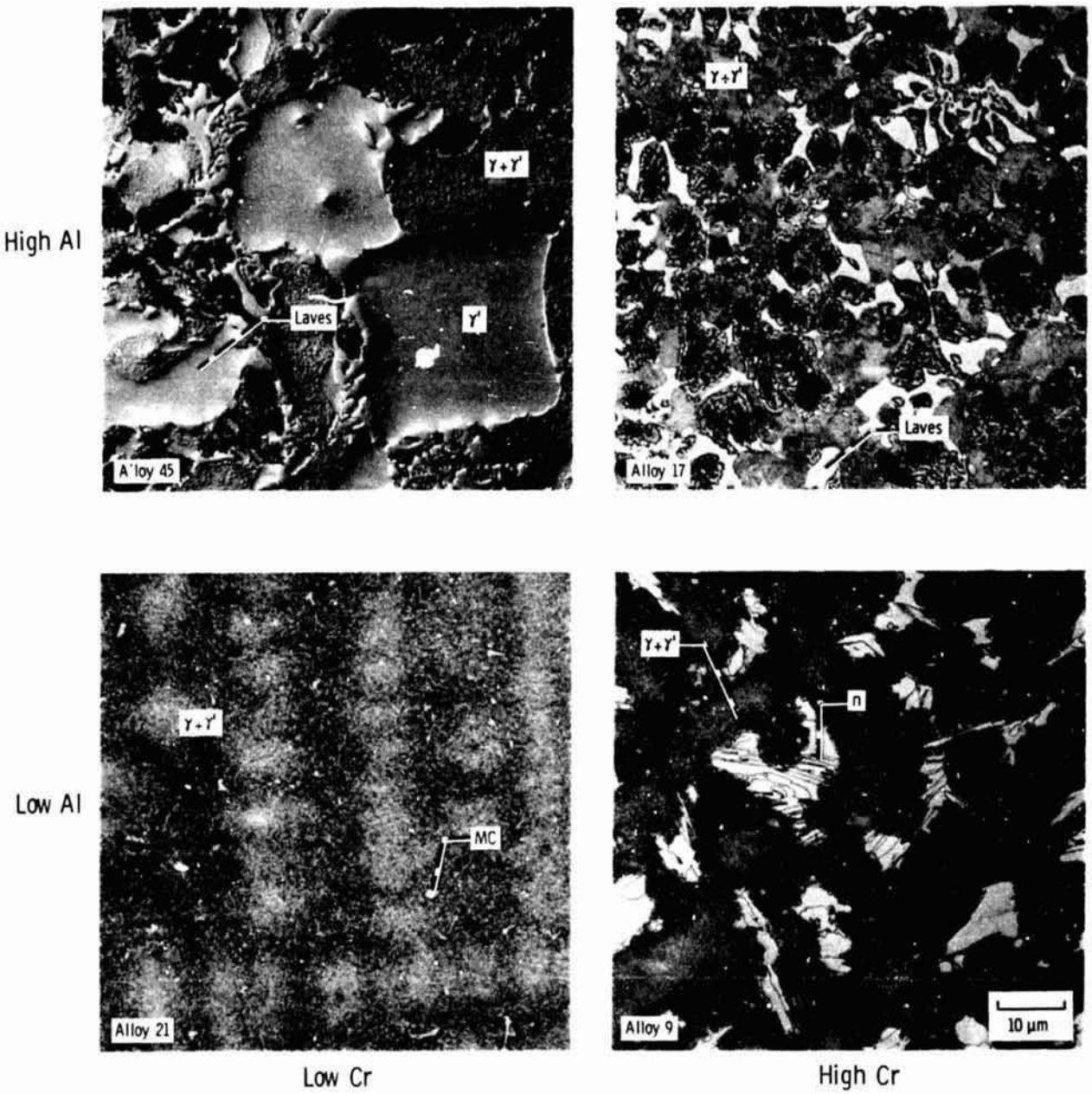

Figure 2. - Optical micrographs of representative as-cast alloys at corner points of experimental design, showing range of microstructures obtained. All alloys tested in as-cast condition.

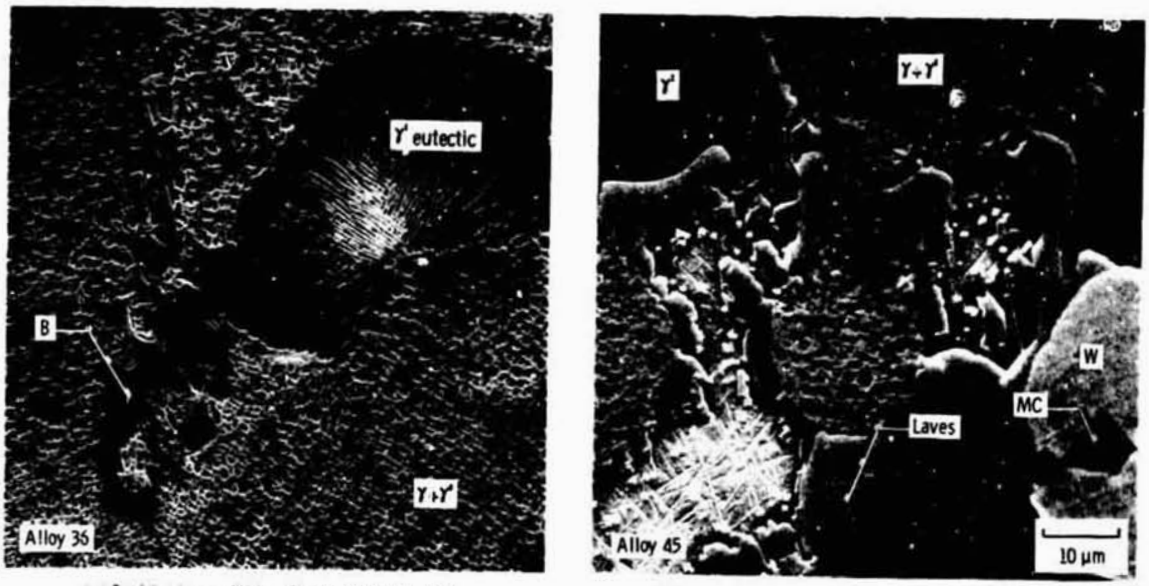

(a) Boride phase, M_3B_2, B (eg. $(CrMoW)_3B_2$).

(b) Laves phase, AB_2, L (eg. $(CrNiCo)(TaNbMoW)_2$). Tungsten phase, W.

Figure 3. - Representative scanning electron micrographs of phases identified by energy dispersive analysis of metallographic specimens and x-ray diffraction of extraction residues.

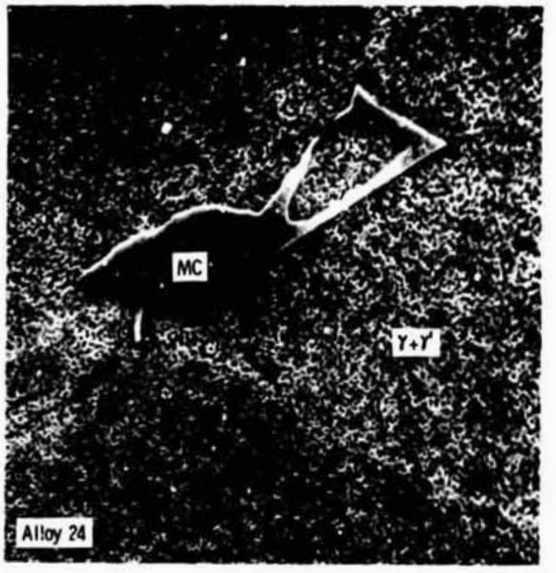

(c) Carbide phase, MC (eg. (TaTiNb) (C, Ni).

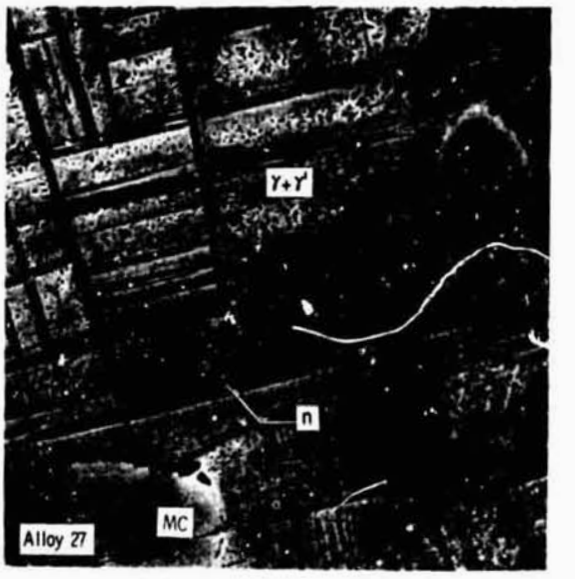

(d) ETA phase, A_3B, η (eg. Ni_3Ti).

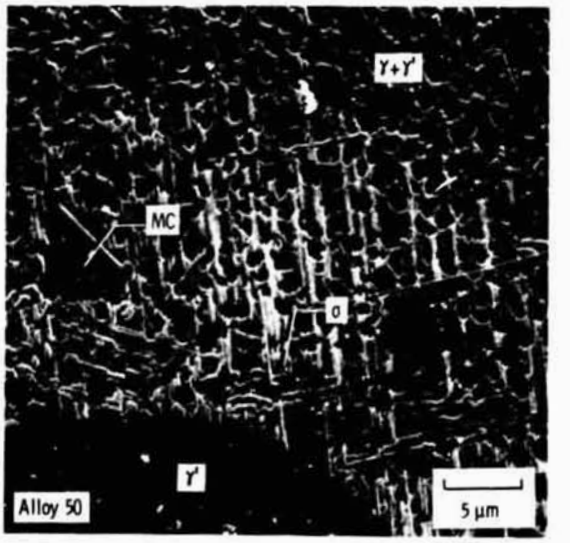

(e) Sigma phase, σ (eg. CrNiMo).

Figure 3. - Concluded.

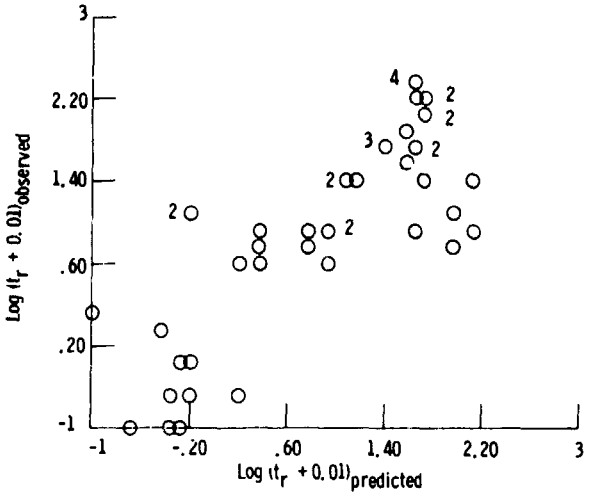

Figure 4. - Plot of predicted versus observed values of log $(t_r + 0.01)$ for stress rupture tests at 1023 K/600 MPa.

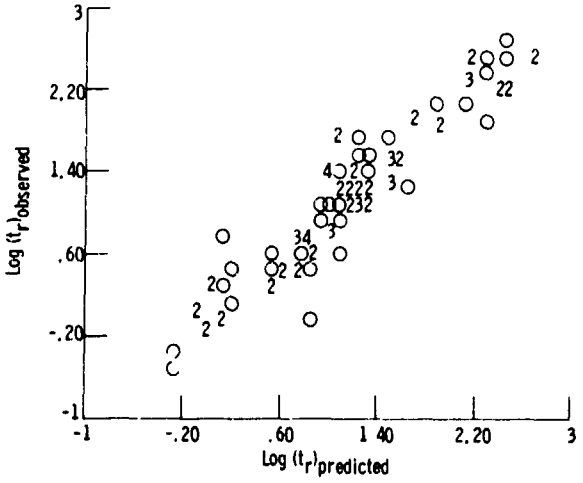

Figure 5. - Plot of predicted versus observed values of log (t_r) for stress rupture tests at 1273 K/600 MPa.